JOURNAL OF SOLID STATE CHEMISTRY 88, 543–554 (1990)

# Defect Solid State Chemistry of Magnetoplumbite-Structured Ceramic Oxides II: Defect Energetics in $LaMgAl_{11}O_{19}$

LIKE XIE AND A. N. CORMACK

*New York State College of Ceramics, Alfred University, Alfred, New York 14802*

Received February 6, 1990; in revised form June 18, 1990

The defect solid state chemistry of $LaMgAl_{11}O_{19}$ has been investigated using computer atomistic simulation techniques. Our calculations show that intrinsic disorder in $LaMgAl_{11}O_{19}$ is of Schottky type. Several defect reactions, proposed to explain the nonstoichiometry of $LaMgAl_{11}O_{19}$, have been modeled; the calculated energies predict that some are much more likely than others. We have also modeled some complexes which have been proposed to form between the spinel blocks in the magnetoplumbite structure. Our results suggest that the nonstoichiometry of $LaMgAl_{11}O_{19}$ may be attributed to these defect complexes which are found to be energetically stable. It is proposed that different complexes will dominate different regions of nonstoichiometry. 

## 1. Introduction

The compound $LaMgAl_{11}O_{19}$ is currently of interest as a high-power laser host (*1, 2*). The first structural analysis of $LaMgAl_{11}O_{19}$ was undertaken by Kahn *et al.* (*1*). Their X-ray diffraction analysis described the structure as a slightly distorted magnetoplumbite phase and is thus related to the ideal magnetoplumbite based on $Al_2O_3$ ($SrAl_{12}O_{19}$), with $La^{3+}$ substituting for $Sr^{2+}$ and $Mg^{2+}$ for one $Al^{3+}$. Our earlier computer atomistic simulations on $SrAl_{12}O_{19}$ indicated that $Mg^{2+}$ ions would prefer to occupy tetrahedral Al sites in the spinel blocks (*3*). To explain the easier preparation of a magnetoplumbite phase when $M^{2+}$ ions, such as $Mg^{2+}$ or $Mn^{2+}$, are present, Gasperin *et al.* (*4*) suggested that the $M^{2+}$ ions could stabilize the spinel blocks by reducing the amount of vacancies in one unit cell. As $Mg^{2+}$ ions are substituted for $Al^{3+}$ ions, to achieve neutrality in $LaMgAl_{11}O_{19}$, it is necessary to consider in detail the nonstoichiometry and defect structures for both the undoped and doped hexa-aluminates containing trivalent cations.

Unlike hexa-aluminates containing monovalent or divalent cations, the structures of which have been extensively investigated, there are only a few studies which are related to the detailed structure of those containing trivalent cations.

Abrahams *et al.* (*5*) claimed that in $LaMgAl_{11}O_{19}$, the principal La site is not fully occupied but contains 4.76 at.% Al and 5.24 at.% Schottky defects. Stevels and Verstegen (*6*) indicated that hexagonal aluminates such as $La_{1-y}Al_{11+(2/3+y)}O_{19}$ and $Ce_{1-y}Al_{11+(2/3+y)}O_{19}$ have a magnetoplumbite structure. Later, mainly based on the luminescence data, Stevels (*7*) proposed a defect structure model in which one oxygen ion is located at the crystallographic position normally occupied by the large trivalent cation such as $La^{3+}$. A further investigation of the crystal structures of hexa-aluminates with trivalent cations was performed by Iyi



0022-4596/90 $3.00

*et al.* (*8*). For $La_{0.827}Al_{11.9}O_{19.09}$, they found interstitial Al ions situated in pairs, making a bridge between the spinel blocks, and causing Al and La defects in the intermediate layer ($z \approx 0.25$). Therefore, they attributed the nonstoichiometry of lanthanum hexa-aluminate to these defects.

It is clear that, because of the complexity of the basic crystal structure of magnetoplumbite-type compounds, the knowledge of the defect structure available from experiment is quite limited. Therefore, we are undertaking a systematic study of the defect structure and nonstoichiometry for magnetoplumbite-structured compounds, using theoretical, computer-based simulation methods. We have shown earlier, in part I (*3*), that transferring interatomic potential parameters from models of binary oxides provides an adequate model of the magnetoplumbite structure. This present work is an extension of the computational methods to more complex structures and stoichiometries than those which have hitherto been investigated.

## 2. Simulation Methods

### *2.1 Defect Energy Calculation*

Calculations of defect structures and energies introduce one vital feature in addition to those for the perfect lattice methods. This is the occurrence of relaxation of lattice atoms around the defect species. The effect is large because the defect generally provides an extensive perturbation of the surrounding lattice, and, in the case of ionic crystals, the relaxation field is long-range as the perturbation provided by the defect is mainly Coulombic in origin.

The theory of defect energy calculation has been outlined by Catlow *et al.* (*9*). Basically, the simulation techniques were based on a generalized Mott–Littleton (*10*) approach developed by Norgett (*11*), where the important feature is that the crystal surrounding the defect is divided into two regions. The outer region II is treated as a polarizable dielectric continuum, while the coordinates of the distorted inner region I are explicitly relaxed using appropriate interatomic potentials. Therefore, we can write the total energy of system $E$ as

$$E = E_1(x) + E_2(x,y) + E_3(y), \qquad (1)$$

in which $E_1$ is the energy of the inner region and thus a function of the coordinates $x$ (and dipole moments) of the ions solely within the region I, $E_3$ depends solely on the displacements $y$ of the ions within II, and $E_2(x,y)$ is due to interaction of regions I and II.

### *2.2 Potential Models*

In our present work, the potentials are assumed essentially ionic and exclusively two body. The lattice energy can be expressed as

$$U = \frac{1}{2}\sum_i \sum_j (q_i q_j / r_{ij} + V_{ij}), \qquad (2)$$

where $r_{ij}$ is the distance between the ions. The first term of Eq. (2) is the long-range coulombic interaction corresponding to the interaction between charges. The second term covers the two-body, short-range, noncoulombic interactions, which are described by a simple analytical Buckingham function,

$$V(ij) = A_{ij}\exp(-r_{ij}/\rho_{ij}) - C_{ij} r_{ij}^{-6}. \qquad (3)$$

The short-range interaction includes both the repulsive forces due to the overlap of ion charge clouds, and an attractive term due to dispersive interactions. The simulation of polarizability in the ions that constitute the lattice is included through the shell model originally developed by Dick and Overhauser (*12*). This model consists of a simple mechanical representation of the ionic dipole. The polarizable valence shell electrons are represented by a mass-less shell which is connected to the core by an harmonic spring. Potential parameters ($A$,

TABLE I

INTERIONIC POTENTIALS

(A) Short-range parameters for potential form $V(r) = Ae^{-r/\rho} - Cr^{-6}$

| Interaction | $A$(eV) | $\rho$(Å) | $C$(eV.Å$^{-6}$) |
|---|---|---|---|
| La–O | 1644.980 | 0.36196 | 0.000 |
| Ce–O | 1771.660 | 0.36000 | 0.000 |
| Mg–O | 1428.500 | 0.29453 | 0.000 |
| Al–O | 1474.400 | 0.30059 | 0.000 |
| O–O | 22764.200 | 0.14910 | 17.890 |

(B) Shell parameters

| Interaction | Shell charge ($Y/e$) | Spring constant $k$(eV.Å$^{-2}$) |
|---|---|---|
| La(Core)–La(Shell) | 3.000 | 99999.99 |
| Ce(Core)–Ce(Shell) | 3.000 | 99999.99 |
| Mg(Core)–Mg(Shell) | 2.000 | 99999.99 |
| Al(Core)–Al(Shell) | 3.000 | 99999.99 |
| O(Core)–O(Shell) | −2.207 | 27.29 |

$\rho$, and $C$), with the appropriate shell charges, $Y$, and spring constant, $K$, were taken from the compilation of Lewis and Catlow (*13*) and are listed in Table I. The short-range potential cutoff, the interatomic separation beyond which the potential is assumed to be negligible for computational convenience, is 1.89 lattice units.

## 3. Results and Discussion

### *3.1 Intrinsic Disorder*

An important point to note is that the defect energies were calculated within our equilibrated crystal structure. The structure reported by Kahn *et al.* (*1*) was used as an initial set up for the calculation. With the X-ray data as the starting point, the program METAPOCS (*14*) was used to minimize the energy of the unit cell with respect to the coordinates of all the ions. All the atomic coordinates within the unit cell (not just the symmetry-independent ones) were allowed to relax in order to find the minimum energy configuration. In this way, we calculated equilibrium positions for atoms in $LaMgAl_{11}O_{19}$, which are reported in Table II.

For $LaMgAl_{11}O_{19}$, vacancy and interstitial formation energies were calculated for each of the possible species; these energies are gathered together in Table III.

From the calculated energies for cation and anion vacancies and interstitials, Schottky and Frenkel defect formation energies may be determined; these are also given in Table III, as energies per constituent defect. Note that because the different types of disorder involve varying numbers of defects, comparison in terms of energy per defect is essential. The thermodynamic grounds for this have been discussed by Catlow and

TABLE II

A COMPARISON OF THE FINAL EQUILIBRATED ATOM POSITIONS WITH THE X-RAY STRUCTURE FOR $LaMgAl_{11}O_{19}$

| Atom | | Data from X-ray structure | Data from calculation | $\Delta^a$ |
|---|---|---|---|---|
| La | $x$ | 0.6667 | 0.6667 | 0.0000 |
| | $z$ | 0.2500 | 0.2500 | 0.0000 |
| Al(1) | $x$ | 0.0000 | 0.0000 | 0.0000 |
| | $z$ | 0.0000 | −0.0019 | 0.0019 |
| Al(2) | $x$ | 0.0000 | 0.0000 | 0.0000 |
| | $z$ | 0.2500 | 0.2500 | 0.0000 |
| Al(Mg)(3) | $x$ | 0.3333 | 0.3333 | 0.0000 |
| | $z$ | 0.0273 | 0.0296 | 0.0023 |
| Al(4) | $x$ | 0.1676 | 0.1671 | 0.0005 |
| | $z$ | −0.1082 | −0.1087 | 0.0005 |
| Al(5) | $x$ | 0.3333 | 0.3333 | 0.0000 |
| | $z$ | 0.1895 | 0.1879 | 0.0016 |
| O(1) | $x$ | 0.0000 | 0.0000 | 0.0000 |
| | $z$ | 0.1499 | 0.1525 | 0.0026 |
| O(2) | $x$ | 0.3333 | 0.3333 | 0.0000 |
| | $z$ | −0.0576 | −0.0595 | 0.0016 |
| O(3) | $x$ | 0.1820 | 0.1830 | 0.0010 |
| | $z$ | 0.2500 | 0.2500 | 0.0000 |
| O(4) | $x$ | 0.1520 | 0.1532 | 0.0012 |
| | $z$ | 0.0530 | 0.0553 | 0.0023 |
| O(5) | $x$ | 0.5050 | 0.5057 | 0.0007 |
| | $z$ | 0.1508 | 0.1502 | 0.0006 |

[a] Difference between equilibrated and X-ray structures.

TABLE III

CALCULATED DEFECT ENERGIES FOR THE BASIC ATOMISTIC DEFECTS

| Defect | Defect energy (eV) |
|---|---|
| $La^{3+}$ vacancy | 31.78 |
| $La^{3+}$ interstitial | −21.39 |
| $Mg^{2+}$ vacancy | 26.23 |
| $Mg^{2+}$ interstitial | −20.06 |
| $Al^{3+}$ vacancy | 52.35 |
| $Al^{3+}$ interstitial | −46.05 |
| $O^{2-}$ vacancy | 21.25 |
| $O^{2-}$ interstitial | −16.23 |
| $La^{3+}$ Frenkel[a] | 5.20 |
| $Al^{3+}$ Frenkel[a] | 3.15 |
| $O^{2-}$ Frenkel[a] | 2.51 |
| $Mg^{2+}$ Frenkel[a] | 3.09 |
| Schottky[a] | 1.94 |

[a] Energy per constituent defect.

TABLE IV

LATTICE ENERGIES OF RELEVANT COMPOUNDS PER FORMULA UNIT

| Compound | Lattice energy (eV) |
|---|---|
| $LaMgAl_{11}O_{19}$ | −975.49 |
| $Al_2O_3$ | −160.31 |
| $La_2O_3$ | −124.00 |
| MgO | −41.18 |

James (*15*). Our results show clearly that the Schottky disorder is the dominant defect mode to be expected in $LaMgAl_{11}O_{19}$. This conclusion is consistent with that made by Abrahams *et al.* (*5*).

### *3.2 Probable Defect Processes Involved in Nonstoichiometric $LaMgAl_{11}O_{19}$*

There are several possible nonstoichiometric formulas related to $LaMgAl_{11}O_{19}$, such as $La_{1-x}MgAl_{11+x}O_{19}$, $LaMg_xAl_{11}O_{18+x}$, $La_{1-x}Al_{11+2/3+x}O_{19}$, $La_{1-x}MgAl_{11+x(2/3+1)}O_{19+x}$, $LaMg_xAl_{11+0.67(1-x)}O_{19}$, and $La_{1-x}Mg_xAl_{11+x+0.67(1-x)}O_{19}$. Each of these different formulas describe different ways in which the nonstoichiometry may be accommodated and each involves a different defect structure. Since the associated defect processes depend on the energetics of the various defect species concerned, we thought it worthwhile to calculate the energies of the various reactions for the different models of nonstoichiometry to see whether a clear favorite emerged. The lattice and defect energies related to defect processes are shown in Tables IV and V. The defect processes, along with their reaction energies, are listed in Table VI.

*Defect process 1: $La_{1-x}MgAl_{11+x}O_{19}$.* For defect process 1, La deficiency is exactly compensated by excess Al leading to the reaction

$$LaMgAl_{11}O_{19} + (x/2)Al_2O_3 \rightarrow La_{1-x}MgAl_{11+x}O_{19} + (x/2)La_2O_3. \quad (4)$$

Therefore, the substitution of $Al^{3+}$ for $La^{3+}$ can lead immediately to a charge balance. However, there are two possible sites, an interstitial position or the $La^{3+}$ site, in which the $Al^{3+}$ might be located. The energies of the defect reactions corresponding to these two cases have been calculated and are labeled $E_1$ for $Al_{La}$compensation and $E_1'$ for $Al_i$ compensation. The lower value calculated for $E_1$ indicates that $Al_{La}$ defects will be preferred. Abrahams *et al.* (*5*) found that all Al (Mg) sites are fully occupied and that the La site contained $(1 - x)$ La and $x$ Al

TABLE V

CALCULATED DEFECT ENERGIES FOR SUBSTITUTION

| Defect | Energy (eV) |
|---|---|
| $Ce_{La}$ | −1.534 |
| $Al_{La}$ | −17.00 |
| $Al_{Mg}$ | −31.20 |

TABLE VI

CALCULATED ENTHALPY FOR DEFECT PROCESSES

Process 1

$LaMgAl_{11}O_{19} + (x/2)Al_2O_3 \rightarrow La_{1-x}MgAl_{11+x}O_{19} + (x/2)La_2O_3$

$E_1 = (1/2)E_{La_2O_3} + E_{Al_{La}} - (1/2)E_{Al_2O_3} = 1.16$ eV

$E'_1 = (1/2)E_{La_2O_3} + E_{V_{La}} + E_{Al_i} - (1/2)E_{Al_2O_3} = 3.89$ eV

Process 2

$LaMgAl_{11}O_{19} \rightarrow LaMg_xAl_{11}O_{18+x} + (1 - x)MgO$

$E_2 = E_{MgO} + E_{V_{Mg}} + E_{V_O} = 6.30$ eV

Process 3(a)

$LaMgAl_{11}O_{19} + (x/2 + 1/3)Al_2O_3 \rightarrow La_{1-x}Al_{11+2/3+x}O_{19} + MgO + (x/2)La_2O_3$

$E_{3a1} = E_{Al_{La}} + 1/3\,E_{V_{Mg}} + 2/3\,E_{Al_{Mg}} + E^{lat}_{MgO} + 1/2\,E^{lat}_{La_2O_3} - 1/2\,E^{lat}_{Al_2O_3} - 1/3\,E^{lat}_{Al_2O_3} = 1.36$ eV

$E_{3a2} = E_{Al_i} + 1/3\,E_{V_{Mg}} + 2/3\,E_{Al_{Mg}} + E^{lat}_{MgO} + 1/2\,E^{lat}_{La_2O_3} - 1/2\,E^{lat}_{Al_2O_3} - 1/3\,E^{lat}_{Al_2O_3} = 4.09$ eV

Process 3(b)

$LaMgAl_{11}O_{19} + (1/2 + 2x/3)Al_2O_3 \rightarrow La_{1-1/3-x/3}Al_{12+x/3}O_{19} + MgO + (1/6 + x/3)La_2O_3$

$E_{3b1} = 2/3\,E_{Al_{La}} + 1/3\,E_{V_{La}} + E_{Al_{Mg}} + E^{lat}_{MgO} + 1/2\,E^{lat}_{La_2O_3} - (1/2 + 1/3)\,E^{lat}_{Al_2O_3} = -1.53$ eV

$E_{3b2} = 2/3\,E_{Al_i} + 2/3\,E_{V_{La}} + 1/3\,E_{V_{La}} + E_{Al_{Mg}} + E^{lat}_{MgO} + 1/2\,E^{lat}_{La_2}O_3 - 5/6\,E^{lat}_{Al_2O_3} = 0.29$ eV

Process 4

$LaMgAl_{11}O_{19} + x(1/2 + 1/3)Al_2O_3 \rightarrow La_{1-x}MgAl_{11+x(2/3+1)}O_{19+x} + (x/2)La_2O_3$

$E_4 = 1/2E_{La_2O_3} + E_{V_{La}} + E_{O_i} + (1 + 2/3)E_{Al_i} - (1/2 + 1/3)E_{Al_2O_3} = 10.19$ eV

Process 5

$LaMgAl_{11}O_{19} + (1 - x)/3Al_2O_3 \rightarrow LaMg_xAl_{11+2/3(1-x)}O_{19} + (1 - x)MgO$

$E_5 = E_{MgO} + E_{V_{Mg}} + 0.67E_{Al_i} - 0.67/2E_{Al_2O_3} = 7.90$ eV

Process 6

$LaMgAl_{11}O_{19} + [x/2 + 0.67(1 - y)/2]Al_2O_3 \rightarrow La_{1-x}Mg_yAl_{11+x+0.67(1-y)}O_{19} + (1 - y)MgO + (x/2)La_2O_3$

$E_6 = E_{1'} + E_5 = 9.06$ eV

atoms. Our simulations are, thus, in good agreement with their conclusion.

*Defect process 2: $LaMg_xAl_{11}O_{18+x}$.* Nonstoichiometric $LaMg_xAl_{11}O_{18+x}$ is deficient in both magnesium and oxygen. This compositional change can be obtained by removal of MgO from $LaMgAl_{11}O_{19}$ and is described by defect process 2 with the reaction

$$LaMgAl_{11}O_{19} \rightarrow LaMg_xAl_{11}O_{19+x} + (1 - x)MgO. \quad (5)$$

The energy for this process is 6.30 eV which is quite large, suggesting that this reaction, by itself, is not likely to occur. Gasperin *et al.* (*4*) prepared and studied a series of compounds with initial composition $LaM_xAl_{11}O_{18+x}$ ($0 \leq x \leq 1$) in order to understand the role of $M^{2+}$ ions in the formation of magnetoplumbite structure. For the case of $x = 1.0$ ($M^{2+} = Mn^{2+}$), they found that the $LaMnAl_{11}O_{19}$ sample did have a well-defined, distorted, magnetoplumbite structure. However, when they continuously lowered $x$, for instance to 0.7, 0.02, and 0.0, partial occupancies and displacements of ions from the La, Al, and O sites in the mirror plane occurred, as revealed by strong diffuse scattering. They suggested that in all nonstoichiometric phases of $LaM_xAl_{11}O_{18+x}$, the charge compensation mechanism would be very complicated.

However, according to defect process 2, charge compensation is not a real problem. The reason behind the partial occupancy and displacement of ions in the mirror plane may, in fact, be ascribed to structural relaxation. When lowering $x$ to 0.0, this means

that two MgO formula units are removed from one unit cell, providing 4 vacancies. The remaining ions in the unit cell will adjust to a new equilibrium position, in the presence of the vacancies. Of course, we cannot eliminate the possibility that other defect processes may also be involved in this nonstoichiometric compound, but, as we shall see below, the creation of other defects, or defect complexes, in the mirror plane, will also be accompanied by structural relaxation around the defect. In fact, the large calculated defect energies strongly imply that other defect processes will be involved in producing this kind of nonstoichiometry.

*Defect process 3:* $La_{1-x}Al_{11+2/3+x}O_{19}$. This process involves, in addition to disorder on the La and Al sites, much as in process 1, the complete removal of Mg and its replacement by Al. Four possible situations need to be considered, two of which involve $Al_{La}$ substitution and two in which the $V_{La}$ are compensated by aluminum interstitials. Stevels and Verstegen (*6*) first considered lanthanum hexa-aluminate ($La_{1-x}Al_{11+2/3+x}O_{19}$) to have the magnetoplumbite structure. Although Dexpert-Ghys *et al.* (*16*) later proposed that $La_{1-x}Al_{11+2/3+x}O_{19}$ was composed of both $\beta$-alumina and magnetoplumbite structural units, Iyi *et al.* (*8*) further confirmed that the structure of lanthanum hexa-aluminate corresponded to a magnetoplumbite structure. They were able to eliminate the possibility that $\beta$-alumina-like cells existed in their specimens. Therefore, during our calculations, we assumed that $La_{1-x}Al_{11+2/3+x}O_{19}$ retained the magnetoplumbite structure. Note, however, that the difference between $\beta$-alumina and magnetoplumbite structures is the ion arrangement in the region between the spinel blocks. Any significant disorder in this region will tend to blur the distinction between the two structure types.

In the process we have labeled 3(a), the magnesium deficiency is compensated completely by $Al_{Mg}$ defects; charge neutrality then requires a concentration of $V_{Mg}$. The lathanum deficiency is compensated either by aluminum interstitials or by $Al_{La}$ defects. Thus, in this process, the lanthanum and magnesium deficiencies are treated independently with separate compensation mechanisms. The defect reaction energies indicate a distinct preference for $Al_{La}$ defects and not for aluminum interstitials.

In process 3(b), the difference is now that all the Mg sites are occupied by Al. The excess positive charge now must be balanced by either $V_{La}$ or $V_{Al}$ defects; the lower formation energy of lanthanum vacancies means these would be preferred. Note that now the two deficiencies of La and Mg are not independent: lanthanum vacancies have been introduced as part of the compensation mechanism for magnesium nonstoichiometry. Our results indicate, however, that in this case too, substitutional $Al_{La}$ defects are more likely than Al interstitial species.

From the energies of the four possible defect reactions, we can see that option 3b1 is clearly favored for defect process 3, and in fact is endothermic, implying that this mode of nonstoichiometry is likely to be spontaneous.

Our results do not suggest that the excess Al ions will enter interstitial positions. However, as we shall see in the next section, the formation of interstitial $Al^{3+}$ ions suggested by other workers is probably a result of defect association.

*Defect process 4:* $La_{1-x}MgAl_{11+5/3x}O_{19+x}$. Amongst other defect processes that have also been proposed for the nonstoichiometry of $LaMgAl_{11}O_{19}$ are some which suggest the existence of excess oxygen. It has been proposed by Stevels (*7*) that such excess oxygen in $La_{1-x}MgAl_{11+5/3x}O_{19+x}$ may be found in "vacant" $La^{3+}$ sites (i.e., that oxygen partially occupies La positions); alternatively, an interstitial position for the oxygen may be preferable. The reaction energy calculated for the interstitial oxygen model is 10.19 eV. Our calculations also indicate

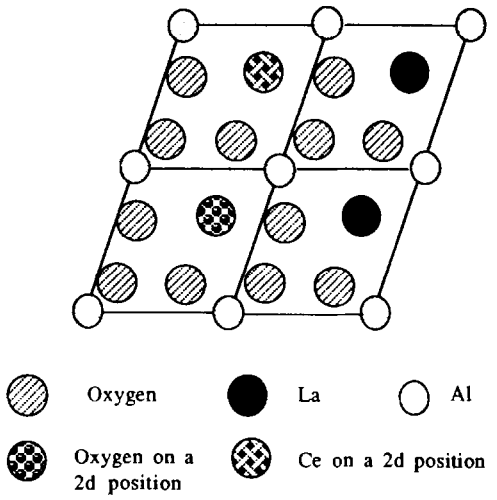


FIG. 1. $xy$ plane at $z = 0.75$ of the magnetoplumbite structure. Four unit cells are shown. An oxygen ion has replaced one La at the 2*d* site and a La has been substituted by Ce.

that it is not favorable for oxygen simply to replace $La^{3+}$, without a substantial rearrangement of its surroundings, as we discuss below. The site potential of the $La^{3+}$ ion positions (as, indeed, for any cation position) usually precludes occupation of that site by a negatively charged ion, so it is not surprising that a simple $O_{La}$ defect should be energetically unfavorable.

Based on luminescence data, Stevels and Verstegen (*6*) constructed a structural model for magnetoplumbite-type materials such as $(La_{0.92},Ce_{0.14})MgAl_{11.33}O_{19}$ and $(Mg_{0.85},Ce_{0.15})Al_{11.95}O_{19}$ in which some of the La or Ce ions are considered to be replaced by excess oxygen. He proposed that the presence of oxygen ions at the 2*d* sites induces a shift of one of the nearby oxygen (6*h*) ions toward a $Ce^{3+}$ ion as seen in Fig. 1. In order to stabilize this O–Ce complex, Al ions in 12*k* sites are also supposed to shift to positions near the $O_{La}$.

Our defect structure calculations support the existence of such an interstitial oxygen model in $LaMgAl_{11}O_{19}$. In our calculations of $LaMgAl_{11}O_{19}$, the interstitial oxygen ions are associated with a larger defect complex, which is discussed in the next section.

*Defect processes 5 and 6.* The possibility that Mg sites become partially vacant and that excess Al enter the structure interstitially is described by process 5. The energies listed in Table VI suggest that excess Al ions prefer to go to interstitial sites with some Mg sites remaining vacant. The large energy of reaction, however, indicates that the process will not occur. Process 6 is a combination of process 1 and process 5. Because this combination causes an increase in energy, this process is also not expected to be energetically favorable.

*Summary.* In general, the nonstoichiometry of the magnetoplumbite structure is very complicated. Defect processes 1 and 3, described above, clearly have the lowest energies and hence may be expected to explain most of the nonstoichiometry in $LaMgAl_{11}O_{19}$. However, as we can see in the next section, a knowledge of defect complexes is crucial since the complexing of defects into aggregates may well alter the energetic balance between the simple defect processes discussed in this section.

### *3.3 Defect Complexes: Structure Models*

The unit cell of the magnetoplumbite structure is composed of two-dimensional slabs perpendicular to the $c$ axis containing four layers of oxygen ions in a cubic close-packed arrangement, with cations, such as $Al^{3+}$, arranged in both octahedral and tetrahedral sites, as in the spinel structure. Two intermediate layers about 11 Å apart contain additional coplanar cations and oxygen ions, which hold the "spinel blocks" together. These intermediate layers are also called mirror planes because of their crystallographic symmetry. Based on this oxygen close packing, it is highly unlikely for defect complexes to exist in the spinel blocks. Therefore, we focus our attention on the

possibilities for defect complexes to form in the mirror plane between the spinel blocks. These defect complexes may be expected to play a key role in the nonstoichiometry of lanthanum hexa-aluminate.

Several possible defect complexes and defect energies are given in Table VII. Our calculations show that the layers between spinel blocks in magnetoplumbite structure have a great flexibility in accommodating defect species, which certainly cause the nonstoichiometry in this structure. Basically, our present study only involves two types of defect models, a "vacancy model" and an "interstitial oxygen model" which we adopted from the models proposed by Iyi *et al.* (*8*) and are shown in Figs. 2a and 2e.

For defect complex 1, a La vacancy, an Al vacancy, and an interstitial Al are associated together, as shown in Fig. 2a. The binding energy of 0.76 eV with respect to isolated, individual defects shows that complex 1 is energetically stable although not by very much. Our calculation also indicates that to stabilize this defect complex, an Al at 2*b* site in the vicinity of interstitial Al ion undergoes a displacement from the 2*b* site (0.0000, 1.0000, 0.7500) in ideal magnetoplumbite structure to a smaller *z* position. Iyi *et al.* (*8*) referred to this type of defect as a "vacancy model."

Our type two defect complex consists of a La vacancy, two 12*k* Al vacancies, and a pair of interstitial Al ions. As shown in Fig. 2b, one interstitial Al ion is above the mirror plane and the other below the mirror plane. Like complex 1, the net charge associated with this complex is $-3$. This complex is found to have a binding energy 3.62 eV. An incorporation of an Al vacancy at the neighboring 2*b* site will further stabilize this defect complex, which is described by complex 3.

From an energetic point of view, oxygen cannot simply occupy a La site: site potentials mitigate against it. In order to stabilize the "*i*O" at La site, there have to exist other interstitials or vacancies; these additional defects in the complex must have the effect of changing the site potential sufficiently to allow the oxygen ion to remain at a site normally occupied by a cation. Iyi *et al.* (*8*) pointed out that, owing to the very large difference in the scattering power between La and oxygen, interstitial oxygens situated at La sites cannot be determined directly by X-ray diffraction. Using atomistic computer simulations, we have modeled defect complexes which are based on the "*i*O model."

When one oxygen occupies the La vacancy in complex 2, defect complex 4 results. The binding energy of this complex is larger than that of complex 2, which indicates that the "*i*O" model is more energetically favorable.

Based on the complex 4, as shown in Fig. 2d, when one Al, at a 2*b* site, which is close to the La site, becomes vacant, complex 5 is constructed. The complex 5 is very similar to the "*i*O" model proposed by Iyi *et al.* (*8*), but the negative binding energy ($-1.46$ eV) suggests that the complex 5 is not energetically stable. The net charge for La site is $-5$ in complex 4. When one Al(2) vacancy ($Z = -3$), which is close to the La site, is added into this complex, the system energy should increase. Thus, it is expected that such a system is not energetically favorable due to the repulsive force between the La site and the Al (2) vacancy and the high net negative charge ($-8$) in the complex 5.

However, in the case of complex 4, when the Al(2) ion is just displaced to an interstitial site, a stable defect cluster (complex 6) is formed, with a large binding energy of 9.86 eV. The complex 6 is a modified "*i*O" model. From the coordinates listed in Table VII, we can see that the interstitial oxygen is not exactly at the La site. At the beginning of calculation, the La site is filled with an interstitial oxygen, but during the calculation, the oxygen ion undergoes a displacement from the La site, indicating that, in

TABLE VII

COORDINATES AND ENERGIES OF DEFECT COMPLEXES IN $LaMgAl_{11}O_{19}$

| Defect complex | Coordinate | | | $E_{defect}$ (eV) | $E_{binding}$ (eV) |
|---|---|---|---|---|---|
| | $x$ | $y$ | $z$ | | |
| Complex 1[a] | | | | 37.32 | 0.76 |
| La vacancy | 0.33333 | 0.66667 | 0.75000 | | |
| Al interstitial | 0.16852 | 0.83146 | 0.80005 | | |
| Al vacancy | 0.16854 | 0.83146 | 0.89319 | | |
| Complex 2 | | | | 40.76 | 3.62 |
| La vacancy | 0.33333 | 0.66667 | 0.75000 | | |
| Al vacancy | 0.16804 | 0.83195 | 0.60914 | | |
| Al interstitial | 0.39014 | 0.81902 | 0.67735 | | |
| Al vacancy | 0.16854 | 0.83146 | 0.89319 | | |
| Al interstitial | 0.39024 | 0.81907 | 0.82321 | | |
| Complex 3 | | | | 91.82 | 4.91 |
| La vacancy | 0.33333 | 0.66667 | 0.75000 | | |
| Al vacancy | 0.16804 | 0.83195 | 0.60914 | | |
| Al interstitial | 0.19565 | 0.38875 | 0.67350 | | |
| Al vacancy | 0.16854 | 0.83146 | 0.89319 | | |
| Al interstitial | 0.19188 | 0.38648 | 0.83001 | | |
| Al vacancy | 0.00000 | 1.00000 | 0.75000 | | |
| Complex 4 | | | | 22.77 | 5.38 |
| La vacancy | 0.33333 | 0.66667 | 0.75000 | | |
| Ox interstitial | 0.19188 | 0.80808 | 0.74060 | | |
| Al vacancy | 0.16804 | 0.83195 | 0.60914 | | |
| Al interstitial | 0.19277 | 0.80726 | 0.66674 | | |
| Al vacancy | 0.16854 | 0.83146 | 0.89319 | | |
| Al interstitial | 0.19723 | 0.80277 | 0.82281 | | |
| Complex 5[b] | | | | 81.96 | −1.46 |
| La vacancy | 0.33333 | 0.66667 | 0.75000 | | |
| Ox interstitial | 0.29877 | 0.70122 | 0.75087 | | |
| Al vacancy | 0.16804 | 0.83195 | 0.60914 | | |
| Al interstitial | 0.17837 | 0.82162 | 0.68906 | | |
| Al vacancy | 0.16854 | 0.83146 | 0.89319 | | |
| Al interstitial | 0.17755 | 0.82245 | 0.81195 | | |
| Al vacancy | 0.00000 | 1.00000 | 0.75000 | | |
| Complex 6 | | | | 24.59 | 9.86 |
| La vacancy | 0.33333 | 0.66667 | 0.75000 | | |
| Ox interstitial | 0.20210 | 0.78964 | 0.76176 | | |
| Al vacancy | 0.16804 | 0.83195 | 0.60914 | | |
| Al interstitial | 0.30383 | 0.69613 | 0.69666 | | |
| Al vacancy | 0.16854 | 0.83146 | 0.89319 | | |
| Al interstitial | 0.17936 | 0.82064 | 0.85050 | | |
| Al vacancy | 0.00000 | 1.00000 | 0.75000 | | |
| Al interstitial | 0.01792 | 0.98208 | 0.73042 | | |

[a] Vacancy model (*8*).
[b] Interstitial model (*8*).

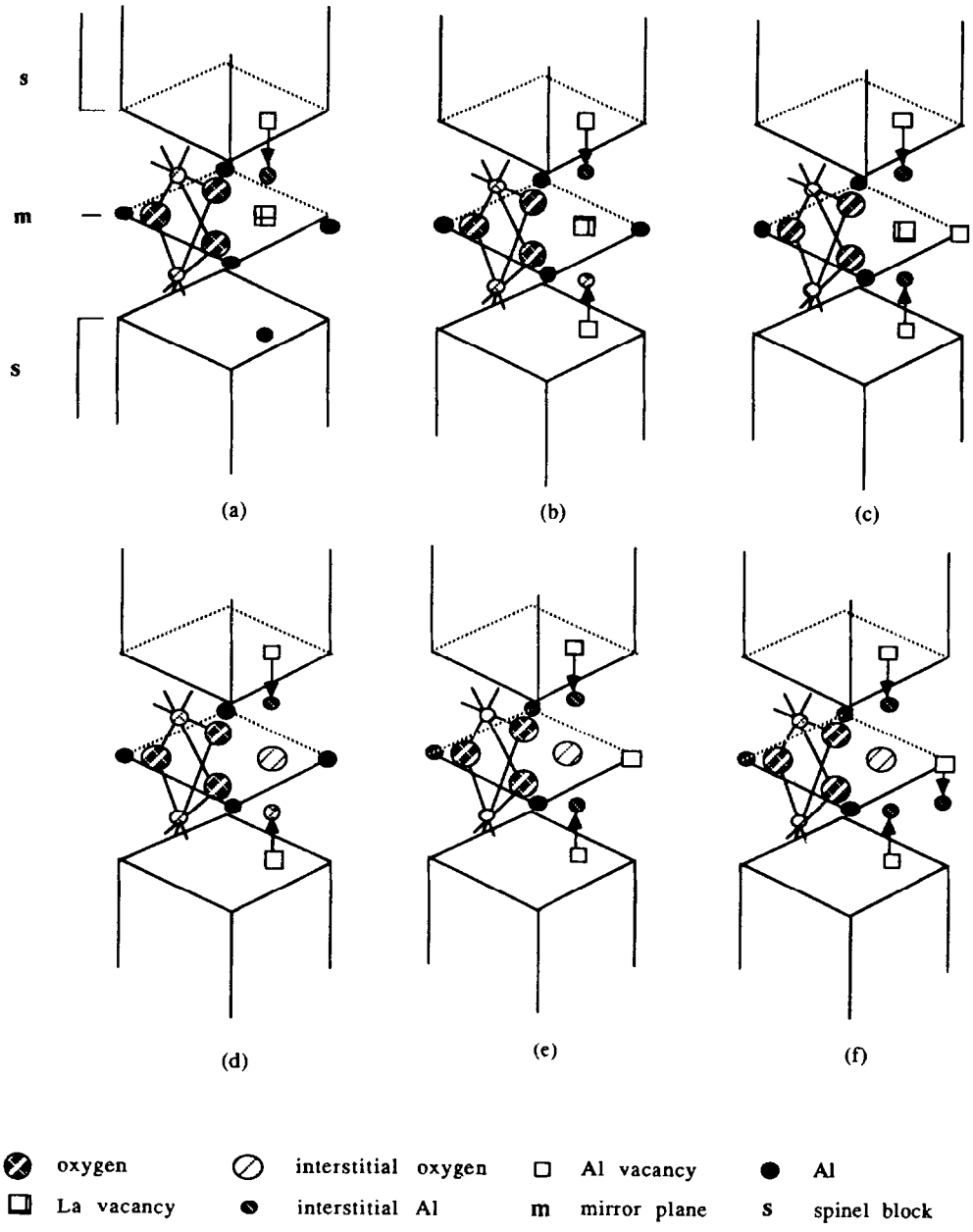


FIG. 2. Five possible types of defect complexes in $LaMgAl_{11}O_{19}$. (a) Type 1: vacancy model. (b) Type 2: the complex of two Al interstitials, two Al vacancies, and one La vacancy. (c) Type 3: the complex of two Al interstitial ions, three Al vacancies, and one La vacancy. (d) Type 4: the complex of two Al vacancies and two Al interstitial ions and one interstitial oxygen (at La site). (e) Type 5: interstitial model. (f) Type 6: modified interstitial model.

such a complex, the interstitial positions also depend on the structure relaxation and charge distribution.

It can also be seen that with an "interstitial" O at the La site, which is associated with Al interstitial ions, the layer between the spinel blocks tends to be a close-packed structure. Iyi *et al.* (*17*) also proposed that such a defect complex can occur in barium $\beta$-alumina, in which one oxygen locates in the conduction plane, with Al interstitials associated with this interstitial oxygen. Therefore, there may be a possibility that the conduction planes become close packed in stabilizing the nonstoichiometric magnetoplumbite or $\beta$-alumina structure.

Although based on the results of refinement and chemical analysis, Iyi *et al.* (*8*) adopted the "vacancy model" to explain the nonstoichiometry of lanthanum hexaaluminate, our calculations indicate that "*i*O model", or at least a simple modification of it, may also be responsible for causing nonstoichiometry in magnetoplumbite structure. Between $LaMgAl_{11}O_{19}$ and $La_{1-x}Al_{11+2/3+x}O_{19}$, there are a lot of variations in composition and thus nonstoichiometry, and the actual defect structure will depend on the details of the nonstoichiometry. For instance, we might use the "vacancy model" for $La_{1-x}MgAl_{11+x}O_{19}$ and the "*i*O model" for $La_{1-x}MgAl_{11+x(2/3+1)}O_{19+x}$. It is also possible that both models may be used to explain the nonstoichiometry in intermediate stoichiometries.

Our simulations suggest that because the layers between the spinel blocks are not close-packed, the defect complex is likely to occur in these layers.

### *3.4 Al(2) Position*

An outstanding controversy in the crystallography of magnetoplumbite structures is whether the [5]-coordinated cation, in this case the Al(2) cation, sits on the mirror plane or is displaced from it. In part I, we examined the effect of moving this ion off the mirror plane, along the *c* direction, looking for a local minimum in site energy. We found none, and concluded that the abnormally large thermal factors which are usually refined for this ion were real and not due to static disorder. However, these calculations were done on a perfect, stoichiometric structure.

We have seen in the structure of the defect complexes discussed in this paper that the Al(2) ion may be absent (the site is vacant in the defect cluster) or at the very least, is displaced away from its mirror plane site, as in complex 1 (Fig. 2a). The displacement of Al(2) from the mirror plane is calculated to be about 0.30 Å, but depends on the type of defect complexes and the position of interstitial ions. Experimentally, in the case of $La_{0.833}Al_{11.833}O_{19.0}$, the distance between the vacant Al(2) 2*b* sites (an ideal position in the magnetoplumbite structure) and the interstitial Al(2) 4*e* sites was found to be 0.25 Å.

Since, in nonstoichiometric samples, the concentration of these defect complexes is likely to be quite large (Iyi *et al.* suggested that one complex in every three or four unit cells would account for compositions of $La_{0.833}Al_{11.833}O_{19.0}$ or $La_{0.875}Al_{11.875}O_{19.125}$), a significant population of the Al(2) ions would be displaced from the mirror plane.

We may say, therefore, that, in contrast to our earlier conclusion based on perfect stoichiometries, the observation of abnormal thermal parameters may be due to static disorder, as a result of the presence of the defect complexes that form to accommodate the nonstoichiometry. We might suggest that these large thermal parameters are an indication of nonstoichiometric disorder and should be absent, or at least minimized, in a perfect stoichiometric and an ideal magnetoplumbite structured crystal.

## 4. Conclusions

In our previous report (*3*), we suggested that intrinsic disorder is of Schottky type in $SrAl_{12}O_{19}$. Here our results further confirm

this conclusion for the stoichiometric magnetoplumbite structure.

As a result of our calculations, we have proposed several feasible defect reactions to explain the nonstoichiometry in $LaMgAl_{11}O_{19}$. In addition, we have modeled some defect complexes which may exist in $LaMgAl_{11}O_{19}$. Although the mirror plane in $LaMgAl_{11}O_{19}$ is more close packed than that in $\beta$-alumina and in $\beta''$-alumina, the layers between the spinel blocks still can accommodate a number of extra ions to lower the energy of the system. The incorporation of a substitutional oxygen onto a lanthanum site is made possible by the formation of defect complexes, in the mirror plane region, which results in a change in La site potential, thus allowing an anion to occupy a cation site, a process which is not normally expected.

Our results show that the nonstoichiometry in $LaMgAl_{11}O_{19}$ (in other magnetoplumbite compounds) may be associated with both the "vacancy model" or the "*i*O model," depending on the type and degree of nonstoichiometry.

## Acknowledgments

We thank the NY State College of Ceramics for financial support. Most of the calculations reported in this work were performed at the Cornell National Supercomputer Facility which is supported in part by New York State, NSF, and IBM corporation. We are also grateful to the referees whose comments allowed us to remove the inconsistencies in our first draft.

## References

1. A. Kahn, A. M. Lejus, M. Madsac, J. Thery, D. Vivien, and J. C. Bernier, *J. Appl. Phys.* **52(11)**, 6864 (1981).
2. D. Vivien, J. Thery, R. Collongues, J. Aubert, R. Moncorge, and F. Auzel, *C. R. Acad. Sci.* **298**, 195 (1983).
3. L. Xie and A. N. Cormack, *J. Solid State Chem.* **83**, 282 (1989).
4. M. Gasperin, M. C. Saine, A. Kahn, F. Laville, and A. M. Lejus, *J. Solid State Chem.* **54**, 61 (1984).
5. S. C. Abrahams, P. Marsh, and C. D. Brandle, *J. Chem. Phys.* **86**, 4221 (1987).
6. A. L. N. Stevels and J. M. P. J. Verstegen, *J. Lumin.* **14**, 207 (1976).
7. A. L. N. Stevels, *J. Electrochem. Soc.* **125**, 588 (1978).
8. N. Iyi, Z. Inoue, S. Takekawa, and S. Kimura, *J. Solid State Chem.* **54**, 70 (1984).
9. C. R. Catlow, R. James, W. C. Mackrodt, and R. F. Stewart, *Phys. Rev. B* **25**, 1006 (1982).
10. N. F. Mott and M. J. Littleton, *Trans. Faraday Soc.* **34**, 485 (1938).
11. M. J. Norgett, Report No. AERE-R7650, A.E.R.E. Harwell, UK (1974).
12. B. G. Dick and A. W. Overhauser, *Phys. Rev.* **112**, 90 (1958).
13. G. V. Lewis and C. R. A. Catlow, *J. Phys. C: Solid State Phys.* **18**, 1149 (1985).
14. C. R. A. Catlow, A. N. Cormack, and F. Theobald, *Acta Crystallogr., Sect. B* **40**, 195 (1984).
15. C. R. A. Catlow and R. James, *Proc. R. Soc. London, Sect. A* **384**, 157 (1982).
16. J. Dexpert-Ghys, M. Faucher, and P. Carro, *J. Solid State Chem.* **41**, 27 (1982).
17. N. Iyi, Z. Inoue, S. Takekawa, and S. Kimura, *J. Solid State Chem.* **52**, 66 (1984).